Title: Sleep need driven oscillation of glutamate synaptic phenotype

Authors: K.E. Vogt [1], A. Kulkarni[2], R. Pandey [3], M. Dehnad[3], G. Konopka[2], R.W. Greene[1,2,3,*]

Affiliations:

1) International Institute of Integrative Sleep Medicine, University of Tsukuba, Tsukuba, Japan

2) Department of Neuroscience, Peter O'Donnell Brain Institute, University of Texas Southwestern Medical Center, Dallas, United States

3) Department of Psychiatry, Peter O'Donnell Brain Institute, University of Texas Southwestern Medical Center, Dallas, United States

* Corresponding author; Email: Robertw.Greene@utsw.edu

Abstract:

Sleep loss increases AMPA-synaptic strength and number in the neocortex. However, this is only part of the synaptic sleep loss response. We report increased AMPA/NMDA EPSC ratio in frontal-cortical pyramidal neurons of layers 2-3. Silent synapses are absent, decreasing the plastic potential to convert silent NMDA to active AMPA synapses. These sleep loss changes are recovered by sleep. Sleep genes are enriched for synaptic shaping cellular components controlling glutamate synapse phenotype, overlap with autism risk genes and are primarily observed in excitatory pyramidal neurons projecting intra-telencephalically. These genes are enriched with genes controlled by the transcription factor, MEF2c and its repressor, HDAC4. Sleep genes can thus provide a framework within which motor learning and training occurs mediated by sleep-dependent oscillation of glutamate-synaptic phenotypes.

Main Text:

CNS control of arousal maintains waking neuronal activities needed for foraging, danger avoidance and reproductive behaviors. Reduction of arousal to unconsciousness can gate sleep, however, the function served by this sleep, in contrast to wake function, remains enigmatic. A reasonable teleologically oriented goal is more effective future foraging, danger avoidance and reproductive behaviors, based on procedural and episodic learning from past waking experience. Effective learning involves memory of waking experience and underlying long-term plasticity (LTP) (Moser et al., 1998; Morris et al., 2003; Stickgold, 2005). At the cellular level, extensive activity dependent LTP of cortical glutamate synapses can lead to a well-documented increase of synaptic strength of cortical glutamatergic synapses during waking. It is reflected by increased frequency and amplitude of glutamatergic miniature synaptic currents (mEPSC) that is restored by subsequent sleep (Liu et al., 2010; Torrado Pacheco et al., 2021), consistent with the synaptic homeostasis hypothesis of sleep (SHY) (Tononi and Cirelli, 2014).

Our recent findings indicate that during waking, not only are individual synapses strengthened (overall glutamate mEPSC amplitude in layer 2-3 pyramidal cells is increased by SD) but, also, the number of electro-physiologically active synapses is increased (increased frequency in correlation with unaltered or decreased probability of release) (Bjorness et al., 2020). The molecular underpinnings of these changes in glutamate synaptic strength and number were examined to determine the changes in the glutamate synaptic phenotype and what the implication(s) of these changes, if any, might be with regards to propensity for synaptic plasticity (meta-plasticity).

We investigated sleep/wake mediated electrophysiological changes in glutamatergic synapses in motor cortex, layer 2-3, pyramidal neurons since our previous work demonstrates wake/sleep up-regulation and down-regulation, respectively, in these cells' glutamate synapses (Bjorness et al., 2020). We observed a wake/sleep oscillation of AMPA/NMDA synaptic response ratio in pyramidal neurons of motor neocortex coupled with an oscillating fraction of silent synapses (NMDAR-mediated synaptic response but no AMPAR mediated response) in response to sleep need. We then, extended these physiological findings to include characterization of sleep-need related differential expression of glutamatergic synaptic shaping genes that can control the observed oscillating glutamate synapse phenotype.

Results

Sleep need driven, glutamate, synaptic phenotype

Three cohorts of C57 BL/6 male mice were allowed either to 1) sleep ad lib (control sleep, CS); 2) prevented from sleeping from ZT=0 to 6h (sleep deprived, SD); or, 3) after 4h SD allowed recovery sleep, ad lib for 2h (RS). *Ex Vivo* acute brain slices from the motor cortex were then prepared from these animals at ZT=6h and

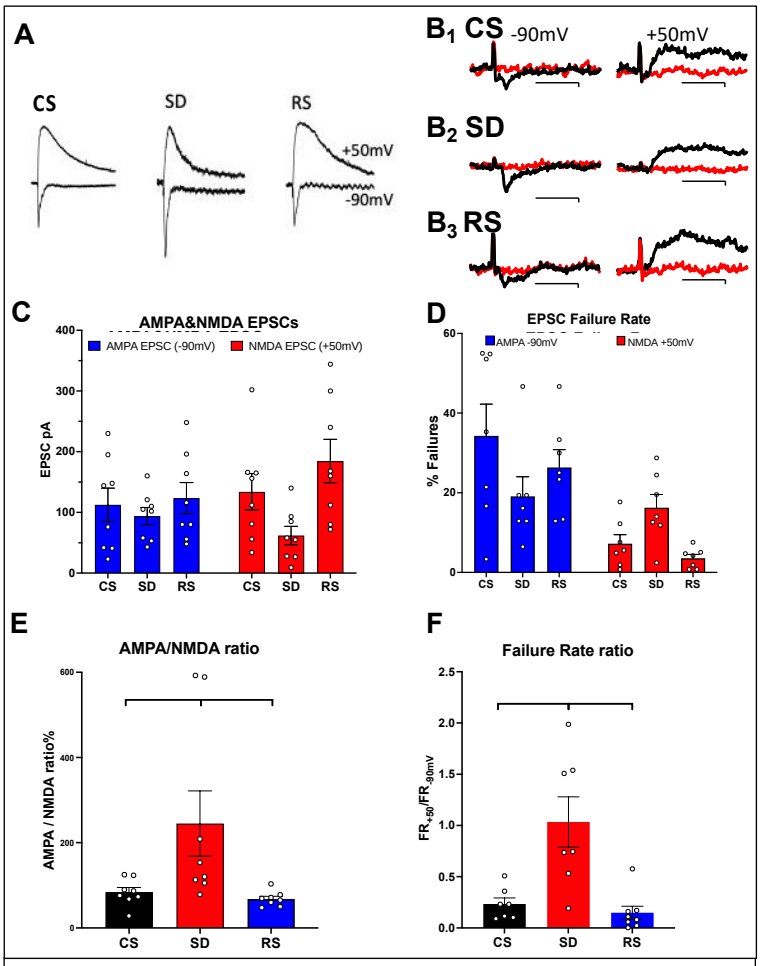

Figure 1. Sleep need-dependent responses of AMPA/NMDA ratio and silent synapses in motor cortex. **A)** Examples of AMPA currents at -90 mV holding potential and NMDA currents at +50 mV holding potential are shown for: control sleep (CS), 6 h of sleep deprivation (SD) and 4 h of sleep deprivation followed by 2 h of recovery sleep (RS). Traces (100msec duration) are scaled to the NMDA current for comparison (NMDA current measured @ 40msec after AMPA peak current). **B)** Examples of successes (black) and failures (red) at -90 mV (left, AMPA) and +50 mV (right, NMDA) after minimal stimulation of excitatory inputs to motor cortex pyramidal neurons are shown; Top row: CS sleep, middle row: SD and bottom row: RS (Cal. 10pAX20msec). Rate of failures (% of all stimuli delivered) for AMPA EPSCs (blue) and NMDA EPSCs (red) in the three conditions (+/- sem). **C), D)** Average (+/- sem) AMPAR and NMDAR EPSC responses (unmatched) and failure rates, respectively, for each sleep condition. **E), F)** Matched AMPA/NMDA EPSC response and AMPA/NMDA failure rate ratios, respectively, are shown for the three conditions (N=1 cell/slice, 2-3 slice/animal, 3 animals/condition).

whole cell recordings obtained from layer 2/3 pyramidal neurons (see methods for details). Locally evoked glutamatergic EPSCs recorded at V_{hold} = -90mV had little NMDAR contribution due to Mg^{++} block. These were compared in the same cell, to EPSCs evoked at V_{hold} = +50mV with little AMPAR contribution due to reduced AMPAR driving force, but, having large NMDAR currents due to voltage sensitive relief from Mg^{++} blockade (NMDAR currents had reversed polarity since E_{NMDAR} =~0mV). For each recorded neuron (one neuron/ slice/ animal) an average response to repeated stimuli (>10 stimuli, 100pA, applied every 10sec) to elicit a EPSC was determined at each holding potential. A two-way ANOVA analysis showed a significant interaction between AMPA matched to NMDA EPSC response for each neuron, and sleep condition ($F(2, 21) = 7.268$, $p<0.004$; Figure 1 A, C, E). When considered independently, neither the effect of sleep condition nor of EPSC subtype reached significance at $p<0.05$ (Figure 1 C).

To control for neuron-to-neuron EPSC variability (due to variability of stimulation-evoked afferent activation), we calculated the AMPA/NMDA ratio, matched for each recorded neuron. This showed a significantly greater AMPA/NMDA EPSC ratio ($F(2, 21) = 3.203$) and comparing SD to CS or RS, $p<=0.03$ or $p<=0.02$, respectively; Dunnett's multiple comparisons test; Table S1, tab 2).

Many glutamatergic synapses on cortical pyramidal cells do not respond to activation at resting membrane potential, yet they do have an NMDAR synaptic component that can be observed at V_{hold}=+50mV. After activation by LTP-evoking stimulation, these 'silent' synapses can convert to active, non-silent

synapses by virtue of LTP-induced AMPAR insertion into the post-synaptic active zone (Liao et al., 1995). The ratio of AMPAR component failure rate (V_{hold}= -90mv; FR_{-90} for active synapses, As) matched with the same neuron's FR_{+50} (V_{hold}= +50mV; for As + silent synapses, Ss) has been used to estimate the change in the fraction of Ss/As in response to LTP (Liao et al., 1995). We employed a similar analysis to examine the effects of SD and sleep on functional synaptic AMPAR and NMDAR composition. We observed a significant interaction between FR's and sleep conditions, assessed by a two-way ANOVA mixed effects model ($F(2, 19) = 5.550$, $p = 0.0126$; Figure 1 $B_{1,2,3}$ D F; Table S1, tab 4). Multiple comparisons revealed no significant difference between FR_{-90} and FR_{+50} in SD indicating far fewer numbers of silent synapses (Ss) in this condition. However, both CS and RS restored the relatively decreased number of Ss compared to SD. FR_{-90} is significantly smaller than FR_{+50} for both CS and RS ($p<0.0001$ and <0.0005, respectively).

The condition specific ratio of FR_{+50mV} to FR_{-90mV} (FRR) is a power function of the probability of failure for each of the stimulated synapses $(1-p_{release})^{stimulated\text{-}synapse}$ and thus, inversely proportional (since $(1-p_{release})<1$) to the number of silent synapses (Ss). A binomial probability distribution model is employed with the assumptions that: 1) each stimulus activates the same set of pre-synaptic terminals for a given neuron; 2) each terminal has a constant $p_{release}$; 3) P(failure) for a given set of stimulus-activated terminals = $(1-p_{release})^{\#activated\ terminals}$. The $FR_{+50mV}/FR_{-90mV} = (1-p_{release})^{As+Ss}/(1-p_{release})^{As}$ and $\ln(FR_{+50mV})/\ln(FR_{-90mV}) =(As+Ss)/As=1+Ss/As$. SD's FR_{+50mV}/FR_{-90mV}=~1 , indicating ~no silent synapses. The FRR of Ss/As for CS=1.44 and for RS=1.46, compared to SD=0.09. The difference between sleep conditions and FRR is significant ($F(2, 19) = 11.3$, Table S1, tab5). Multiple comparisons (Holm-Sidak, Table S1, tab5) indicate the near absence of silent synapses was reversed by either CS or RS (SDxCS; $p<0.0011$ and SDxRS: $p<0.0006$; Table S1, tab 5; Figure 1 F). This suggests there are few if any silent synapses available for conversion by LTP to active synapses following SD and this availability is recovered by sleep.

The sleep-dependent electrophysiological findings raise several questions, including: 1) are other cell types besides the layer 2-3 pyramidal neurons from which we recorded, involved; 2) can changes in the transcriptome account, at least in part, for sleep-related synaptic changes in function, and if so, what are the specific functions of those genes and 3) what is the upstream sleep-dependent control of changes in gene expression?

Cell type/subtype specific gene expression in response to sleep loss

To examine the molecular mechanisms responsible for an SD response, we characterized single nuclei transcriptomes of cells from motor cortex of mice from two cohorts, an ad lib or control sleep (CS) group and an SD group (sleep deprived from ZT= 0-6hr; see detailed methods).

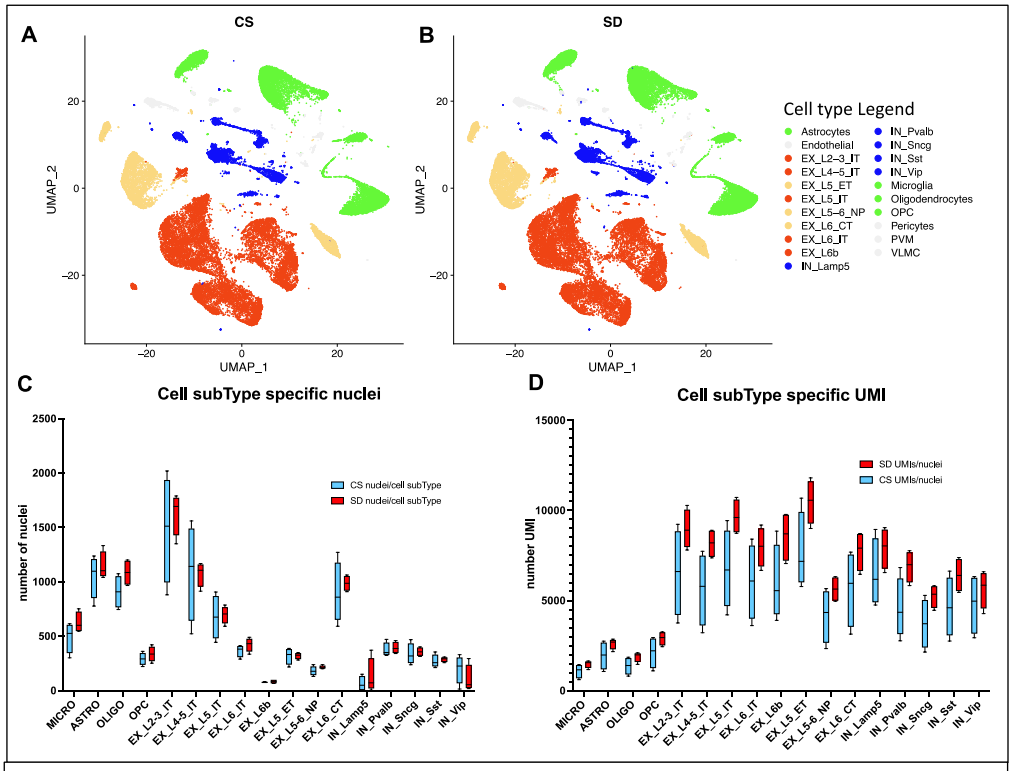

Fig. 2 snRNAseq data shows cell type and sub-type based on gene expression patterns are unaffected by sleep need. **A)** UMAP projection of cell-type gene expression pattern following 6 hours ad lib sleep (CS) at ZT=6hour. **B)** As in "**A**" except after 6hours sleep deprivation (SD), ZT=6hour. **C)** The distribution of cell numbers across subtypes is unaffected by sleep need. **D)** The median number of UMIs/cell is significantly increased by sleep need across all cell subtypes (see_Table S2 and text for statistics).

Transcript libraries from each of the two cohorts (CS, n=4 and SD, n=4), were prepared from single nuclei isolated from mouse frontal cortex. Nuclei from each cohort were clustered and visualized using Uniform Manifold Approximation and Projection (UMAP) and annotated using multi-modal characteristics from the Brain Initiative Cell Census(Network, 2021) (Fig. 2 A,B). The sleep condition had no significant effect on the expression-based clustering nor on the distribution and numbers of nuclei per cell sub-type across sleep conditions (Fig. 2 C). However, the SD condition was associated with a significantly increased number of transcripts/nucleus across sleep condition, matched for cell subtype (2way ANOVA, UMI/Nucleus(subType) x Condition(CSvsSD), $F(16, 96) = 3.004$, $p=0.0004$; Wilcoxon matched-pairs, $p<= 0.0001$; Table S2; Fig. 2 D). To avoid any technical biases, the CS and SD biological samples were treated in an identical manner, with sacrifice alternating between CS and SD samples, carried out by the same person, brain harvesting and frontal cortex isolation all carried out by Dr. Richa Pandey (blinded as to sample identity), RIN values were indistinguishable and finally, library preparation and sequencing were all completed in a single batch. Thus, the results may be indicative of a generalized increase in transcript number per cell sub-type.

We next determined the differential gene expression (DGE) of transcripts between conditions of CS and SD

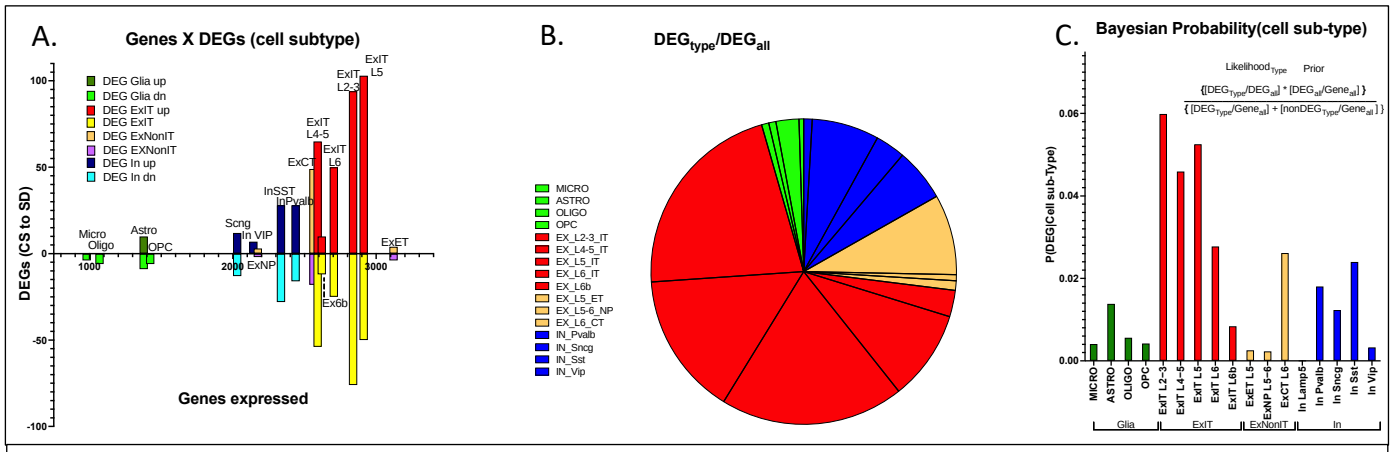

Fig. 3 Cell type specific differential gene expression in response to 6 hours of SD. **A)** An XY bar plot of cell type specific DEGs (both up and down regulated) organized by cell type specific number of expressed genes (X axis) shows the greatest number of DEGs are found in excitatory pyramidal neurons that project within the telencephalon (ExIT). **B)** A pie chart of the distribution of DEGs amongst different cell types illustrates that the majority of sleep DEGs are expressed by ExIT neurons. **C)** An analysis of the cell type specific DEG occurrence shows the greatest probability of significant sleep loss gene response is found in ExIT cells by more than 3-fold compared to all other cell types.

(see methods; Fig. 3 A). In response to 6 hours of SD from ZT= 0 to 6, both increased and decreased gene expression was observed in all cell subtypes (Table S2, S3). Predictably, there is a trend for increased DEGs in cell types expressing a greater number of genes (Fig. 3 A). The greatest proportion of sleep DEGs is ~69%, expressed by ExIT cell types, while the next largest proportion is ~17% for IN cell types (Fig. 3 B). To determine whether the increased numbers of genes expressed in the ExIT subtypes accounts for this cell type's high proportion of DEGs, we examined each cell type's probability of DEG expression given the number of genes expressed in the cell type, its Bayesian probability of expression.

The Bayesian probability of sleep loss DEGs, for cell subtype, is more than three-fold greater for excitatory intratelencephalically projecting neurons (ExIT subtype, pyramidal cells (Network, 2021)) compared to any other class of cells (Fig. 3 C). These observations suggest, with respect to transcriptomic mediated changes in the frontal cortex, the ExIT class neurons comprise the major target of sleep function and extends earlier observations that frontal glutamatergic neurons are the primary targets of the SD transcriptomic response (Bjorness et al., 2020; Kim et al., 2022).

We determined the functional relevance of cell-type specific DEGs with respect to both disease risk and biological properties. We found class-selective enrichment of both autism spectrum disorder genes (ASD;

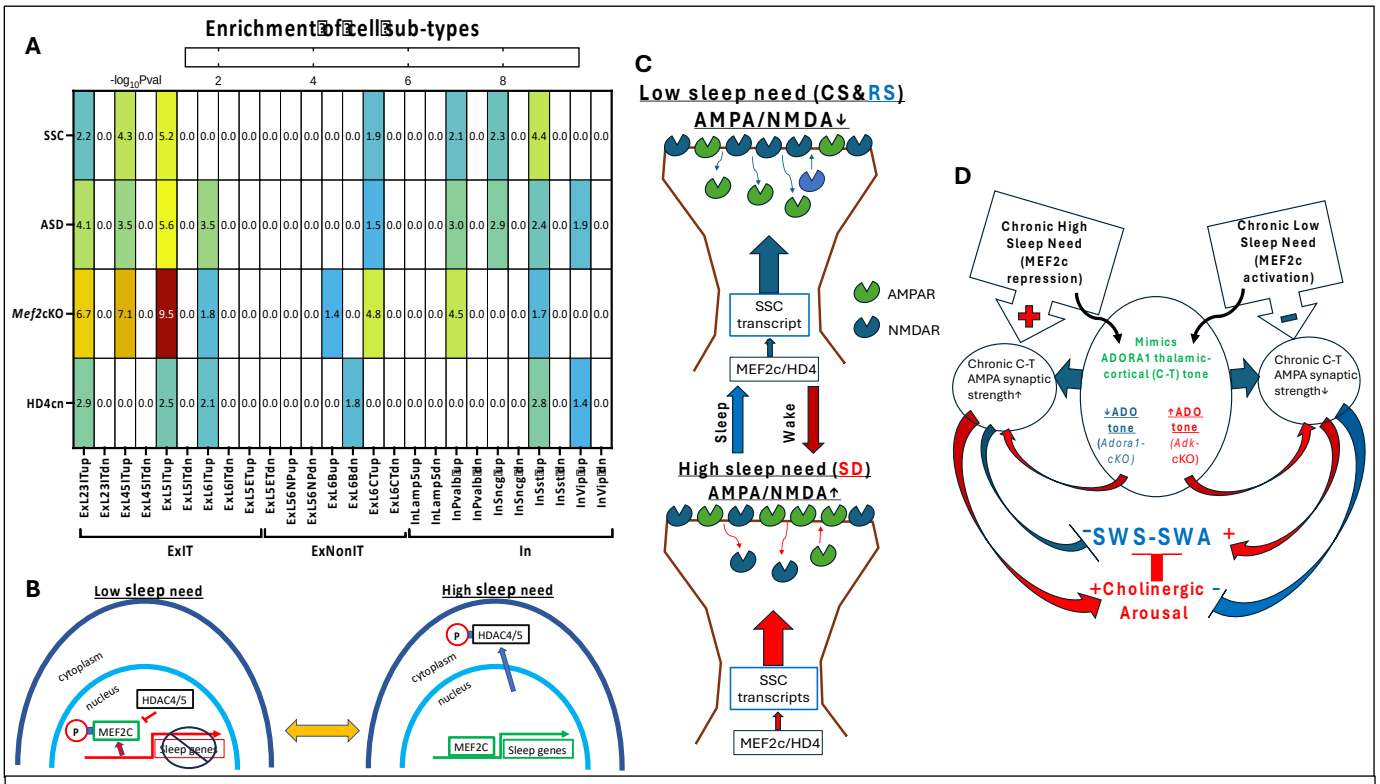

Fig. 4 DEG enrichment of cell types in response to SD by autism risk genes, synaptic shaping component genes and DEGs from *MEF2c* loss of function or constitutive HD4 repression of MEF2c. **A)** Heat map for cell type DEG enrichment by ASD risk genes, Synaptic Shaping Component genes, *MEF2c*-cKO DEGs and HD4cn DEGs. **B)** Model for the control of sleep DEGs by HD4 repression of MEF2c and by pMEF2c during low sleep need and, during high sleep need, de-repression of MEF2c by sequestration of pHD4 to the cytoplasm and dephosphorylation of MEF2c, facilitating expression of sleep genes. **C)** Model of downstream control by MEF2c and HD4 to facilitate SSC gene expression as sleep need increases. The SSC gene expression after waking, can then decrease AMPA/NMDA ratio and increase silent synapses during sleep to bias glutamate synapses towards decreased strength but increased potential for LTP at the start of the active phase when sleep need is low. **D)** An illustration of the SWS-SWA response to chronic MEF2c repression or activation. Chronic activation of MEF2c facilitated transcription leads to decreased AMPAR-mediated synaptic strength mimicking increased Ado tone that inhibits cortical-thalamic, glutamate synaptic activity, decreasing activation of cholinergic arousal centers and increasing SWS-SWA. Chronic repression of MEF2c does the opposite, mimicking loss of ADORA1 function and decreasing SWS-SWA.

Fig. 4 A) and synaptic shaping components (Koopmans et al., 2019) (Fig. 4 A.).

Enrichment of sleep responsive DEGs by SSC and ASD genes, is strongest for ExIT (L 2-3, 4-5, 5) pyramidal neurons (Chi square with Yates correction $p<0.006$). In particular, a number of these sleep need ExIT-DEGs encode proteins that can directly affect AMPA/NMDA ratio and silent synapse numbers, including *Dcc* (Horn et al., 2013), *Dgkb* (Kakefuda et al., 2016), *Gpc6* (Sato et al., 2016), *Grin3a* (Perez-

Otano et al., 2016), *Kif17* (Setou et al., 2000; Iwata et al., 2020), *Kirrl3* (Martin et al., 2015) *and Ptprf* (Sclip and Sudhof, 2020). Some sleep modulated SSCs are also ASD risk factors in frontal cortical EXIT pyramidal neurons, including *Cdh13, Dcc, Glra2, Gpc6, Grik4, Itpr1, Kirrel3, Nr1d1, Pcdh15* and *Ush2a*. To a much lesser extent, Layer 6 corticothalamic pyramidal neurons and somatostatin, parvalbumin and *Sncg* classes of inhibitory neurons (Scala et al., 2021) also show this enrichment of their sleep DEGs (Figure 4 A). These observations are consistent with the ExIT pyramidal cell, glutamatergic, synaptic phenotype as a major functional target for sleep proteins and implicates sleep (dis-)function's role in autism risk.

The transcription factor, MEF2c is necessary for sleep loss gene expression (Bjorness et al., 2020). ExIT sleep loss genes are significantly ($p<0.0001$, Chi^2 with Yates correction) enriched with MEF2c target genes (Harrington et al., 2016; Bjorness et al., 2020) (Figure 4 A.). Class II histone deacetylases 4/5 (HD4, HD5) are MEF2c binding partners and repressors (McKinsey et al., 2000), that can shuttle in and out of the nucleus and are trapped in the cytoplasm when phosphorylated by SIKinases (salt induced kinases (Kim et al., 2022; Zhou et al., 2022)), known to become active in conditions of high sleep need. As the mouse sleep phase progresses, HD4/5 is progressively de-phosphorylated in association with decreased sleep need and conversely as the mouse active phase progress, HD4/5 is progressively phosphorylated in association with increased sleep need (see Figure 4 in Zhou, et al. (Zhou et al., 2022)). A virally-mediated expression of mutant form of HD4, that resists phosphorylation and is thus at constitutively high levels in the nucleus (*HD4cn* (Zhou et al., 2022)), is expected to mimic a loss of function of *MEF2c* through constitutive repression of MEF2c. The sleep loss genes observed in frontal cortical ExIT neurons are enriched for both conditional *Mef2c* (Bjorness et al., 2020) loss of function DEGs ($p<0.0001$, Chi^2 with Yates correction) and for DEGs in response to expression of *HD4cn* (Zhou et al., 2022) ($p<0.0001$, Chi^2 with Yates correction), as illustrated in a sleep-transcriptome expression model (Figure 4 B.). Further, these findings are indicative of the role of HD4 as a repressor of MEF2c facilitated sleep gene expression when sleep need is low and its de-repression of MEF2c through phosphorylation induced sequestration into the cytoplasm when sleep need is high (Zhou et al., 2022). The resulting high-sleep-need DEGs as noted above, can mediate the observed recovery of glutamate synapse phenotype from a high AMPA/NMDA ratio with sparse silent synapses, to lowered AMPA/NMDA ratio and increased silent synapses (Fig. 4 C).

Discussion

Prolonged waking is associated with increased glutamatergic synaptic strength (Vyazovskiy et al., 2008; Liu et al., 2010; Bjorness et al., 2020) and increased number of functional AMPAR synapses (Bjorness et al., 2020). Both effects are reversed by recovery sleep (Bjorness et al., 2020). The evidence presented here suggests this wake/sleep homeostasis also reflects a waking induced increase in functional AMPA/NMDA ratio of glutamate synapses of the frontal cortex together with loss of silent glutamatergic synapses. The latter suggests a reduced availability of glutamate synapses for conversion from silent to active, reflecting saturation of LTP. Accordingly, it is reasonable to summarize the implications of sleep-related glutamate synaptic phenotype oscillation as: 1) prolonged waking induces a generalized synaptic strengthening coupled with a negative bias against potentiating plasticity as available slots for AMPARs saturate, and 2) a recovery by sleep (Fig. 4 C).

Learning of motor tasks that can be robustly and quantitatively monitored, like bird song in juvenile zebra finches (Deregnaucourt et al., 2005; Kollmorgen et al., 2020), may reflect the sleep/wake oscillation of bias for LTP and synaptic strengthening. At the start of the active phase, facilitated motor learning improves song performance to a level that appears to saturate by the end of the day. After a night's sleep, performance is degraded but shows enhanced learning, facilitated by decreased AMPA/NMDA ratio and increased availability of synapses that can be readily potentiated. Since there are inevitable, day to day, unrelated variances in the environment that should not be learned, mitigation of over-fitting a learned task may require an oscillatory, stairstep-like, learning process. In rats, performance during learning of a novel motor task can display these similar characteristics, especially at the start of learning a novel task when exploration of a multi-dimensional learning space is at a premium (Kim et al., 2023), consistent with an underlying sleep/wake oscillation of glutamate synaptic phenotype.

Our unbiased examination of the ontology of ExIT DEGs indicates a response to sleep loss to modify ExIT glutamate synapses involves SSC DEGs. Our electrophysiological observations, now show more particularly, that the gene-expression modifications of ExIT neurons are coupled to SD-responses of, 1) increased AMPA/NMDA ratio; 2) decreased functional silent synapses and; 3) the previously described, increase in synaptic strength and functional number (Fig. 1 and 4).

The ontology of the ExIT SD-response transcriptome is also notable for enrichment by autism-related risk genes, many of which overlap with our curated category of SSCs. A similar overlap has been noted for social affiliative behaviors, synaptic adhesion molecules, other synaptic shaping molecules with autism/autism spectrum disorder (ASD) risk genes in the mammalian CNS (Taylor et al., 2020). The association of sleep disruption with autism is generally appreciated (Mazurek et al., 2019) but the focus was on loss of time spent asleep or disrupted sleep, rather than loss of sleep function. The overlapped SSC and ASD DEGs provide a molecular association between sleep's functional role in motor cortex and ASD risk that captures ASD's association with motor deficits observed in patients (Chukoskie et al., 2013) and in mouse autism models (Cording and Bateup, 2023).

The molecular mechanisms responsible for sleep/wake DEGs observed in ExIT neurons include two critical transcription factors, MEF2c (Bjorness et al., 2020) and HD4/5 (Kim et al., 2022; Zhou et al., 2022). All neuronal and non-neuronal frontal cortical transcriptomic changes are abolished by loss of function of *Mef2c* (Bjorness et al., 2020). The abolishment of the sleep transcriptome remained even after restriction of the *Mef2c* knockout to *CamKII*-expressing glutamatergic neurons of the forebrain. Importantly, MEF2c was necessary for both the SD-transcriptomic response and for SD-induced increase of glutamatergic synaptic strength and functional synaptic number as well as for ensuing sleep-mediated recovery (Bjorness et al., 2020) . Thus, MEF2c has an essential role in facilitating the expression of sleep genes needed for functional recovery from loss of sleep.

The activity of either of these factors to alter the sleep transcriptome, is controlled by their phosphorylation state. When sleep need is high, MEF2c is de-phosphorylated (Bjorness et al., 2020) (from pMEF2c to MEF2c) and Salt Induced Kinases (SIKs) phosphorylate HD4 and HD5 (pHD4/5), sequestering them to the cytoplasm (Kim et al., 2022; Zhou et al., 2022). Both the phosphorylation of HD4/5s (Miska et al., 1999) and de-phosphorylation of MEF2c (Zhu and Gulick, 2004), de-represses MEF2c transcriptional activity. The

de-repression of MEF2c and its dephosphorylation are essential for SD-induced differential expression (Bjorness et al., 2020). The target genes of MEF2c activation can be inferred from the cortical, differential transcriptome induced by MEF2c loss of function (Harrington et al., 2016). These same genes overlap with the differentially expressed genes observed in response to overexpression of constitutively nuclear HD4 (HD4cn). This is predictable as HD4cn will constitutively bind and repress MEF2c in the nucleus, thus mimicking a MEF2c loss of function. Furthermore, in association with low sleep need, nuclear, and thus transcriptionally active (as a repressor), HD4, is more abundant in a de-phosphorylated state, relative to transcriptionally inactive, phosphorylated cytoplasmic pHD4 (Kim et al., 2022; Zhou et al., 2022). NMDAR activation negatively controls HD4 transcriptional activity and nuclear localization (Sando et al., 2012). Accordingly, as NMDAR activity accumulates during the active period, an expected accumulation of pHD4 in the cytoplasm occurs to derepress MEF2c activity. Thus, HD4 may act to repress MEF2c transcriptional facilitation of sleep genes, during low sleep need and derepress MEF2c as sleep need builds during the active period. We observed DEGs from both MEF2c loss of function and HD4cn also sleep DEGs consistent with their interaction driven by sleep need (Figure 4 C).

Both the role of MEF2c to mediate sleep gene expression and nuclear HD4 to repress MEF2c activity, lead to an apparent paradox. When HD4 repression of MEF2c is chronically reduced or lost, sleep need, as indicated by slow wave activity during slow wave sleep (SWS-SWA), is increased (Kim et al., 2022). If MEF2c promotes sleep gene expression, then sleep need should be reduced not increased by its de-repression. Conversely, when constitutively, nuclear HD4 is overexpressed, to chronically repress MEF2c, sleep need, as indicated by SWS-SWA, is unexpectedly, reduced (Zhou et al., 2022). But, what is actually being indicated by SWS-SWA?

SWS-SWA has long been employed as a marker for sleep need or intensity, primarily because of its strong correlation with previous time spent awake (Franken et al., 2001; Borbely et al., 2016). Despite this marker's long history, the mechanisms responsible for its correlation to sleep need are not well understood. A likely candidate is adenosine (Ado) since, it is increased by sleep-need and is necessary for SWS-SWA rebound in response to SD (Porkka-Heiskanen et al., 1997; Bjorness et al., 2009; Bjorness et al., 2016). Ado is increased by glutamate synaptic activity acting on NMDARs in arousal centers. Ado activation of Ado A1 receptors (ADORA1) inhibits AMPAR synaptic activity (Brambilla et al., 2005; Greene et al., 2017). *Adk*, which encodes adenosine kinase in glial cells is the high affinity metabolizing enzyme of Ado. Glial knockout of *Adk* increases extracellular Ado and SWA in both wake and sleep (Bjorness et al., 2016). Rebound SWS-SWA in response to experimental SD increases Ado (Porkka-Heiskanen et al., 1997) and the rebound is blocked by a *CamKII:Cre* driven conditional knockout of *Adora1* (Bjorness et al., 2016). Thus Ado tone, whether increased by prolonged waking activity or by glial knockdown of *Adk*, through its activation of ADORA1, inhibits glutamate synaptic activity, including in arousal centers, to promote SWS-SWA (Greene et al., 2017) (Figure 4 D).

Sleep, itself, induces a down-regulation of glutamate synaptic strength, synaptic numbers, and AMPA/NMDA ratio. Chronic facilitation of MEF2c-dependent sleep genes due to de-repression of MEF2c by HD4/5's loss of function should induce a chronic down-regulation of glutamatergic synaptic strength and number (Bjorness et al., 2020; Kim et al., 2022; Zhou et al., 2022). The sleep-gene induced, chronic glutamate

synaptic down-regulation can mimic the effect of a tonic increase of extracellular Ado to increase SWA as occurred following glial loss of function of *Adk* (Bjorness et al., 2016). Furthermore, synaptic glutamate activity in cholinergic arousal centers (Rainnie et al., 1994; Brambilla et al., 2005) can be reduced, decreasing cholinergic mediated thalamo-cortical activation, and increasing SWS-SWA.

Conversely, repression of MEF2c by de-phosphorylated HD4/5 (or by expression of phospho-dead HD4cn) reduces SWS-SWA (Zhou et al., 2022). In this case, glutamate synaptic activity is chronically increased (directly increasing C-T activation and indirectly driving cholinergic arousal center activity) by the direct effect of loss of sleep function, as evidenced by a loss of function of *Mef2c* in glutamate neurons that prevents sleep gene expression (Bjorness et al., 2020). This prevents the normal down-regulation of glutamate synaptic function (Bjorness et al., 2020) and can mimic the effect of a loss of *Adora1* function on SWS-SWA (Bjorness et al., 2009). It predicts HD4cn's repressive effect on sleep gene expression in response to SD, consistent with the enrichment of SD genes by both HD4cn and *Mef2c*-cKO DEGs, that we observed (Fig. 4 A).

Generally, facilitation or depression of SWA correlates with up or down scaling effects on cortical glutamate neurotransmission, respectively, even in the absence of a direct effects on sleep need (Figure 4D). Many reagents that reduce the excitability of glutamate pyramidal cells by various mechanisms, including anesthetics like isoflurane, barbiturates or benzodiazepines in addition to those activating ADORA1, increase SWA. Those agents that increase excitability of cortical glutamate pyramidal neurons, correlate with decreased SWA. Accordingly, SWA can be a marker for glutamate synaptic strength and number, modulated under normal conditions, by sleep function.

In summary, at the end of a long episode of waking, when sleep need is high, glutamate synapses of ExIT cells in the frontal cortex are electro-physiologically strengthened, increased in functional number, and show increased AMPA/NMDA ratio, together with decreased availability of silent synapses. The silent synapse conversion by LTP to active synapses is thus limited, creating a bias for increased strength at the expense of potentiating plasticity. In the ExIT neuronal nuclei, the transcription factor, MEF2c is de-repressed by de-phosphorylation and sequestration of its co-repressors, the classII HDACs, pHD4/5, to the cytoplasm. This facilitates transcription of sleep genes, including those encoding SSCs controlling glutamatergic synaptic phenotype and ASD risk genes. Recovery sleep recovers the functional phenotype. These observations suggest a daily oscillation from lowered glutamatergic synaptic strength and increased bias for potentiating plasticity at the start of the active phase when sleep need is low, to increased synaptic strength and saturated plasticity at the end of the active phase, when sleep need is high. In conclusion, we have provided electrophysiological evidence for a wake/sleep oscillation of glutamate synapse phenotype that can mediate a glutamatergic strength/plasticity oscillating bias. We also show that this wake/sleep oscillation is likely to occur in glutamate synapses of ExIT pyramidal neurons and be mediated by a select set of synaptic shaping component genes, a significant number of which are also autism risk genes, whose expression is controlled by MEF2C and HD4 transcription factors. Finally, this study implicates a framework within which optimal cortical-dependent motor training can occur in a recursive incremental manner, facilitated by wake/sleep glutamate synapse phenotypical oscillation.

Materials and Methods

Electrophysiology:

All electrophysiological animal experiments were approved by the Animal Experimental Committee at the University of Tsukuba. Animals were housed on a 12:12-h light/dark cycle (with the light automatically turned on at 9:00) at a stable temperature (24.5 ± 0.5 °C), with free access to food and water. C57/Bl6 male mice aged 8 to 12 weeks were used.

Slice preparation and recording:

Mice were fully anesthetized at ZT 6 with isoflurane, and their brains were promptly removed (<1 min) and placed in ice-cold artificial cerebrospinal fluid (ACSF), composed of 124 mM NaCl, 26 mM NaHCO3, 3mM KCl, 2 mM CaCl, 1 mM MgSO4, 1.25 mM KH2PO4, 10 mM glucose, 300 to 310 mOsm, equilibrated with 95% O2 and 5% CO2.

Brains were mounted on the stage of a vibrating microtome (Leica VT1200 S) with cyanoacrylate glue. Coronal sections (300 µm thick) were obtained and allowed to recover in ACSF at room temperature for at least 1 h. Slices were submerged in a perfusion chamber placed under an upright microscope (BX51WI; Olympus) fitted with a custom LED IR illumination and Nomarski interference contrast. Slices were superfused with ACSF, at a rate of 2 mL/min with Picrotoxin (100 micromolar) added to block GABAA receptor-mediated responses. Neurons in layers 2/3 of primary motor cortex with a pyramidal cell morphology were patched under visual control. The intracellular solution contained (in mM) 130 Cs gluconate, 1 mM EGTA, 10 mM Hepes, 4 mM MgATP, 0.3 mM NaGTP, and 5 mM NaCl. The pH was adjusted to 7.33 with CsOH and osmolarity to 285 to 300 mOsm. Borosilicate patch pipettes were pulled to an open-tip resistance of 2 to 4 MΩ. Signals were amplified and filtered at 10 kHz (Axopatch 700A; Molecular Devices) and then digitized at 20 kHz using customized routines in commercial software (IGORPro; WaveMetrics). Series resistance values for the recording pipette ranged between 8 and 15 MOhm and experiments with changes larger than 25% were not used for further analyses.

Evoked synaptic responses were produced through extracellular stimulation (0.1 ms) every 10 s with monopolar glass pipette electrodes filled with ACSF and placed in the vicinity (200-400 micrometers) lateral to the recorded neuron in layer 2/3. For the AMPA/NMDA amplitude ratio experiments stimuli amplitudes were 8.7 uA +/- 3.5 uA (SD) and for the failure rate experiments, 1.4 uA +/-0.9 uA (SD).

AMPA/NMDA EPSC analyses:

AMPA responses were recorded at a holding potential of -90 mV and mixed AMPA-NMDA responses at a holding potential of +50 mV. The -90 mV holding potential was chosen according to precedent (Myme et al., 2003). The hyperpolarized holding potential increases driving force and permits lower stimulus strength for the same response size – reducing the likelihood for polysynaptic responses. Experiments with multiple response peaks at -90 mV were not included in the analysis. The -90 mV holding potential also increases NMDA receptor Mg block - resulting in a minimally contaminated AMPA response.

The AMPA/NMDA ratio was determined according to an established protocol (Myme et al., 2003); briefly, at least 10 traces were averaged at -90 mV and +50 mV, the AMPA response was calculated as the peak inward current at -90 mV and the NMDA current was calculated at +50mV in a 5 ms window 40 ms after the AMPA peak.

Failure rates for AMPA and AMPA+NMDA EPSCs: Minimal stimulation was achieved by lowering the stimulation strength until clear successes and failures could be observed at -90 mV holding potential and stimulation strength was then kept constant for 5-10 min to allow the system to stabilize before failure ratios were determined. Relative numbers of silent and total (silent + active) synapse in an L2-3 pyramidal neuron evoked in a slice by minimal presynaptic stimulation are correlated with failure rates (FR= failures/number of stimuli). FR-90 = (1-prelease)As, and FR+50 = (1-prelease)As+Ss, where As=number active synapses (at -90mV) and Ss= number of silent synapses (only active at +50mV). Since prelease for each synapse is the same for -90mV and +50mV (i.e., assuming the same probability of failure at both potentials with each stimulus) then:

ln(FR+50) = ln (1-prelease)As+Ss

= (As+Ss)*ln(1-prelease)

ln(FR-90)= ln(1-prelease)As

=As*ln(pfailure)

Thus,

ln(FR+50)/ln(FR-90) = (As+Ss)/As

=1 + Ss/As.

Since (FR+50/FR-90)= (1-prelease)As+Ss / (1-prelease)As, as Ss-->0, (FR+50/FR-90)--> 1, the maximum ratio possible if prelease is constant. Our uncorrected data show (FR+50/FR-90)=~1.3 in SD, which suggests that FR+50 is overestimated by at least a factor of 1.3 (likely, due to decreased input resistance at Vh=+50mV). Accordingly, we adjusted FR+50 by this factor = 1.3, for all sleep conditions.

Sleep deprivation

All mice were accommodated for 1-2 weeks to a cage and treadmill, consisting of a bottomless plexiglass enclosure suspended over the treadmill with ad lib access to food and water. During this time, all animals were exposed to treadmill movement at ZT=2 and ZT=14 hours, for 30 minutes. For sleep deprivation (SD) the slow-moving treadmill (SMTM; 0.1KM/hour; see “video 1”) was engaged from ZT 0-6 hours and for recovery sleep (RS) from ZT 0-4. There was no treadmill engagement for RS from ZT 4-6 hours and for control sleep (CS), no treadmill engagement for the entire ZT 0-6 hours period. All animals were sacrificed at ZT=6 hours and tissue rapidly prepared for either electrophysiological (exVivo brain slices) or transcriptomic analysis as described below.

Single nucleus Transcriptome analysis:

snRNA-seq library preparation:

Nuclei for snRNA-seq were isolated from male mice, 8-10 weeks old. Briefly, the tissue was homogenized using a glass Dounce homogenizer in 2 ml of ice-cold lysis buffer (10 mM Tris-HCl, 10 mM NaCl, 3 mM MgCl2 and 0.1% Nonidet P40 Substitute) and was incubated on ice for 5 min. Nuclei were centrifuged at 500g for 5 min at 4 °C, washed with 4 ml ice-cold lysis buffer and incubated on ice for 5 min. Nuclei were centrifuged at 500g for 5 min at 4 °C. After centrifugation, the nuclei were resuspended in 500 µl of nucleus suspension buffer (NSB) containing 1× PBS, 1% BSA (no. AM2618, Thermo Fisher Scientific) and 0.2 U µl−1 RNAse inhibitor (no. AM2694, Thermo Fisher Scientific). The nucleus suspension was filtered through a 70-µm Flowmi cell strainer (no. H13680-0070, Bel-Art). Debris was removed with density gradient centrifugation using Nuclei PURE 2 M sucrose cushion solution and Nuclei PURE sucrose cushion buffer from the Nuclei PURE prep isolation kit (no. NUC201-1KT, Sigma Aldrich). Nuclei PURE 2 M sucrose cushion solution and Nuclei PURE sucrose cushion buffer were first mixed in a 9:1 ratio. A 500 µl volume of the resulting sucrose solution was added to a 2-ml Eppendorf tube. A 900 µl volume of the sucrose buffer was added to 500 µl of isolated nuclei in NSB. A 1,400 µl volume of nucleus suspension was layered to the top of the sucrose buffer. This gradient was centrifuged at 13,000g for 45 min at 4 °C. The pellet of nuclei was resuspended, washed once in NSB and filtered through a 70-µm Flowmi cell strainer (no. H13680-0070, Bel-Art). The concentration of nuclei was determined using 0.4% trypan blue (no. 15250061, Thermo Fisher Scientific), and was adjusted to a final concentration of 1,000 nuclei per microlitre with NSB.

Droplet-based snRNA-seq libraries were prepared using Chromium Single Cell 3′ v3.1 (1000121, 10x Genomics) according to the manufacturer’s protocol(Zheng et al., 2017). Libraries were sequenced using an Illumina NovaSeq 6000. snRNA-seq preprocessing and annotationRaw sequencing data was obtained as BCL files from the McDermott sequencing core at UT Southewestern. BCL files were demultiplexed using cellranger mkfastq (10X Genomics CellRanger suite v3.1.0). Resulting FASTQ files were then accessed for quality using FASTQC (v0.11.5). A reference mouse genome-annotation index was built for mouse genome (GRCm38p6) and Gencode annotation (vM17) using cellranger mkref (10X Genomics CellRanger suite v3.1.0). Quality passed FASTQ files were further aligned to reference mouse genome-annotation index and raw count matrices were generated using cellranger count (10X Genomics CellRanger suite v3.1.0). To remove ambient RNA contamination, we used CellBender’s remove-background (https://github.com/broadinstitute/CellBender) on the raw count matrix per sample. We note that without

ambient RNA removal, glial cells were shown to be conspicuously contaminated with neuronal ambient RNAs(Caglayan et al., 2022). Also, potential doublets were discarded using DoubletFinder (https://github.com/chris-mcginnis-ucsf/DoubletFinder) tool. Ambient RNA and doublets cleaned data were used for downstream analysis. For each sample, nuclei with less than 20,000 UMIs and percentage of reads mapping to mitochondrial genes of less then 0.5 were retained. Individual samples per sleep condition were first integrated using Seurat's (v3) integration approach (IntegrateData) and integrated datasets were further clustered (ScaleData, RunPCA, FindClusters) as described in Seurat's (v3) integration vignette (https://satijalab.org/seurat/archive/v3.0/integration). Clustered data was then visualized (RunUMAP) using Uniform manifold approximation and projection embeddings (UMAP). Cluster-specific gene markers were identified (FindMarkers) and significant marker genes were enriched using Fisher exact test for cell-type markers defined in Brain Initiative Cell Census to annotate the cell-types. Cell-types were also confirmed by expression of canonical marker genes.

Differential gene expression tests were performed using edgeR-based pseudobulk approach across sleep conditions per cell-type. Significant differentially expressed genes (DEGs) were identified using absolute log2 fold change >= 0.1375 (10%) and a false discovery rate (FDR) <= 0.05. Further significant DEGs were enriched across defined gene classes (such as SSC genes, ASD genes, Mef2c-cKO genes and HD4cn genes) using R package SuperExactTest to functionally annotate the genes.

Statistics

The exact sample size (n) for each experimental group/condition, is provided as a discrete number and unit of measurement. Statistics were taken from distinct samples and not measured repeatedly, with the exception of the matched sampled evoked EPSCs recorded at Vh=-90mV and at Vh=+50mV from the same neuron as part of the analyses of AMPAR and NMDAR EPSC amplitudes and failure rates. Statistical details are provided in appropriate tables (Tables 1-3) in tabs labelled "Stats ….", in the "Supplementary Information-Data/Tables".

References and Notes

Bjorness TE, Kelly CL, Gao T, Poffenberger V, Greene RW (2009) Control and function of the homeostatic sleep response by adenosine A1 receptors. The Journal of neuroscience : the official journal of the Society for Neuroscience 29:1267-1276.

Bjorness TE, Dale N, Mettlach G, Sonneborn A, Sahin B, Fienberg AA, Yanagisawa M, Bibb JA, Greene RW (2016) An Adenosine-Mediated Glial-Neuronal Circuit for Homeostatic Sleep. The Journal of neuroscience : the official journal of the Society for Neuroscience 36:3709-3721.

Bjorness TE, Kulkarni A, Rybalchenko V, Suzuki A, Bridges C, Harrington AJ, Cowan CW, Takahashi JS, Konopka G, Greene RW (2020) An essential role for MEF2C in the cortical response to loss of sleep in mice. Elife 9.

Borbely AA, Daan S, Wirz-Justice A, Deboer T (2016) The two-process model of sleep regulation: a reappraisal. J Sleep Res 25:131-143.

Brambilla D, Chapman D, Greene R (2005) Adenosine mediation of presynaptic feedback inhibition of glutamate release. Neuron 46:275-283.

Chukoskie L, Townsend J, Westerfield M (2013) Motor skill in autism spectrum disorders: a subcortical view. International review of neurobiology 113:207-249.

Cording KR, Bateup HS (2023) Altered motor learning and coordination in mouse models of autism spectrum disorder. Front Cell Neurosci 17:1270489.

Deregnaucourt S, Mitra PP, Feher O, Pytte C, Tchernichovski O (2005) How sleep affects the developmental learning of bird song. Nature 433:710-716.

Franken P, Chollet D, Tafti M (2001) The homeostatic regulation of sleep need is under genetic control. JNeurosci 21:2610-2621.

Greene RW, Bjorness TE, Suzuki A (2017) The adenosine-mediated, neuronal-glial, homeostatic sleep response. Current opinion in neurobiology 44:236-242.

Harrington AJ, Raissi A, Rajkovich K, Berto S, Kumar J, Molinaro G, Raduazzo J, Guo Y, Loerwald K, Konopka G, Huber KM, Cowan CW (2016) MEF2C regulates cortical inhibitory and excitatory synapses and behaviors relevant to neurodevelopmental disorders. Elife 5.

Horn KE, Glasgow SD, Gobert D, Bull SJ, Luk T, Girgis J, Tremblay ME, McEachern D, Bouchard JF, Haber M, Hamel E, Krimpenfort P, Murai KK, Berns A, Doucet G, Chapman CA, Ruthazer ES, Kennedy TE (2013) DCC expression by neurons regulates synaptic plasticity in the adult brain. Cell reports 3:173-185.

Iwata S, Morikawa M, Takei Y, Hirokawa N (2020) An activity-dependent local transport regulation via degradation and synthesis of KIF17 underlying cognitive flexibility. Sci Adv 6.

Kakefuda K, Ishisaka M, Tsuruma K, Shimazawa M, Hara H (2016) Memantine, an NMDA receptor antagonist, improves working memory deficits in DGKbeta knockout mice. Neurosci Lett 630:228-232.

Kim J, Joshi A, Frank L, Ganguly K (2023) Cortical-hippocampal coupling during manifold exploration in motor cortex. Nature 613:103-110.

Kim SJ et al. (2022) Kinase signalling in excitatory neurons regulates sleep quantity and depth. Nature 612:512-518.

Kollmorgen S, Hahnloser RHR, Mante V (2020) Nearest neighbours reveal fast and slow components of motor learning. Nature 577:526-530.

Koopmans F et al. (2019) SynGO: An Evidence-Based, Expert-Curated Knowledge Base for the Synapse. Neuron 103:217-234 e214.

Liao D, Hessler NA, Malinow R (1995) Activation of postsynaptically silent synapses during pairing-induced LTP in CA1 region of hippocampal slice. Nature 375:400-404.
Liu ZW, Faraguna U, Cirelli C, Tononi G, Gao XB (2010) Direct evidence for wake-related increases and sleep-related decreases in synaptic strength in rodent cortex. The Journal of neuroscience : the official journal of the Society for Neuroscience 30:8671-8675.
Martin EA, Muralidhar S, Wang Z, Cervantes DC, Basu R, Taylor MR, Hunter J, Cutforth T, Wilke SA, Ghosh A, Williams ME (2015) The intellectual disability gene Kirrel3 regulates target-specific mossy fiber synapse development in the hippocampus. Elife 4:e09395.
Mazurek MO, Dovgan K, Neumeyer AM, Malow BA (2019) Course and Predictors of Sleep and Co-occurring Problems in Children with Autism Spectrum Disorder. J Autism Dev Disord 49:2101-2115.
McKinsey TA, Zhang CL, Lu J, Olson EN (2000) Signal-dependent nuclear export of a histone deacetylase regulates muscle differentiation. Nature 408:106-111.
Miska EA, Karlsson C, Langley E, Nielsen SJ, Pines J, Kouzarides T (1999) HDAC4 deacetylase associates with and represses the MEF2 transcription factor. The EMBO journal 18:5099-5107.
Morris RG, Moser EI, Riedel G, Martin SJ, Sandin J, Day M, O'Carroll C (2003) Elements of a neurobiological theory of the hippocampus: the role of activity-dependent synaptic plasticity in memory. PhilosTransRSocLond B BiolSci 358:773-786.
Moser EI, Krobert KA, Moser MB, Morris RG (1998) Impaired spatial learning after saturation of long-term potentiation. Science 281:2038-2042.
Myme CI, Sugino K, Turrigiano GG, Nelson SB (2003) The NMDA-to-AMPA ratio at synapses onto layer 2/3 pyramidal neurons is conserved across prefrontal and visual cortices. Journal of neurophysiology 90:771-779.
Network BICC (2021) A multimodal cell census and atlas of the mammalian primary motor cortex. Nature 598:86-102.
Perez-Otano I, Larsen RS, Wesseling JF (2016) Emerging roles of GluN3-containing NMDA receptors in the CNS. Nat Rev Neurosci 17:623-635.
Porkka-Heiskanen T, Strecker RE, Thakkar M, Bjorkum AA, Greene RW, McCarley RW (1997) Adenosine: a mediator of the sleep-inducing effects of prolonged wakefulness. Science 276:1265-1268.
Rainnie DG, Grunze HC, McCarley RW, Greene RW (1994) Adenosine inhibition of mesopontine cholinergic neurons: implications for EEG arousal. Science 263:689-692.
Sando R, 3rd, Gounko N, Pieraut S, Liao L, Yates J, 3rd, Maximov A (2012) HDAC4 governs a transcriptional program essential for synaptic plasticity and memory. Cell 151:821-834.
Sato K, Takahashi K, Shigemoto-Mogami Y, Chujo K, Sekino Y (2016) Glypican 6 Enhances N-Methyl-D-Aspartate Receptor Function in Human-Induced Pluripotent Stem Cell-Derived Neurons. Front Cell Neurosci 10:259.
Scala F, Kobak D, Bernabucci M, Bernaerts Y, Cadwell CR, Castro JR, Hartmanis L, Jiang X, Laturnus S, Miranda E, Mulherkar S, Tan ZH, Yao Z, Zeng H, Sandberg R, Berens P, Tolias AS (2021) Phenotypic variation of transcriptomic cell types in mouse motor cortex. Nature 598:144-150.
Sclip A, Sudhof TC (2020) LAR receptor phospho-tyrosine phosphatases regulate NMDA-receptor responses. Elife 9.
Setou M, Nakagawa T, Seog DH, Hirokawa N (2000) Kinesin superfamily motor protein KIF17 and mLin-10 in NMDA receptor-containing vesicle transport. Science 288:1796-1802.
Stickgold R (2005) Sleep-dependent memory consolidation. Nature 437:1272-1278.

Taylor SC, Ferri SL, Grewal M, Smernoff Z, Bucan M, Weiner JA, Abel T, Brodkin ES (2020) The Role of Synaptic Cell Adhesion Molecules and Associated Scaffolding Proteins in Social Affiliative Behaviors. Biol Psychiatry 88:442-451.

Tononi G, Cirelli C (2014) Sleep and the price of plasticity: from synaptic and cellular homeostasis to memory consolidation and integration. Neuron 81:12-34.

Torrado Pacheco A, Bottorff J, Gao Y, Turrigiano GG (2021) Sleep Promotes Downward Firing Rate Homeostasis. Neuron 109:530-544 e536.

Vyazovskiy VV, Cirelli C, Pfister-Genskow M, Faraguna U, Tononi G (2008) Molecular and electrophysiological evidence for net synaptic potentiation in wake and depression in sleep. NatNeurosci 11:200-208.

Zhou R et al. (2022) A signalling pathway for transcriptional regulation of sleep amount in mice. Nature 612:519-527.

Zhu B, Gulick T (2004) Phosphorylation and alternative pre-mRNA splicing converge to regulate myocyte enhancer factor 2C activity. Mol Cell Biol 24:8264-8275.

Acknowledgments: Dr. Theresa Bjorness discussed and helped edit the manuscript.

Funding support was provided by:

National Institute of Neurological Disorders and Stroke NS103422 to Robert W Greene

National Institute on Deafness and Other Communication Disorders DC014702 to Genevieve Konopka

James S. McDonnell Foundation 220020467 to Genevieve Konopka

International Institute for Integrative Sleep medicine and by AMED under Grant Number JP21zf0127005 to Kaspar Vogt.

Author contributions:

Conceptualization: RWG

Methodology: KEV, AK, MD, RP

Investigation: RWG, AK, MD, RP

Visualization: RWG, KEV, AK

Project administration: RWG

Supervision: RWG, KEV

Writing – original draft: RWG

Writing – review & editing: RWG, AK, GK

Competing interests: There are no competing.

Data and materials availability:

Data availability

Raw and processed data are available at National Center for Biotechnology Information GEO under the accession number **GSE256140** at https://www.ncbi.nlm.nih.gov/geo/query/acc.cgi?acc=GSE256140 .

Code availability Statement

All analysis scripts are available at https://github.com/konopkalab/sleep_need_seq .